

# **Hyperspectral image classification based on multi-scale residual network with attention mechanism**

Xiangdong Zhang, Tengjun Wang, and Yun Yang

*College of Geological Engineering and Geomatics, Chang'an University, Xi'an, China*

Xiangdong Zhang, xiangdong2018@chd.edu.cn, College of Geological Engineering and Geomatics, Chang'an University, Xi'an, China

# Hyperspectral image classification based on multi-scale residual network with attention mechanism

Compared with traditional machine learning methods, deep learning methods such as convolutional neural networks (CNNs) have achieved great success in the hyperspectral image (HSI) classification task. HSI contain abundant spatial and spectral information, but they also contain a lot of invalid information, which may introduce noises and weaken the performance of CNNs. In order to make full use of the useful information in HSI, we propose a multi-scale residual network integrated with attention mechanism (MSRN-A) for HSI classification in this letter. In our method, we built two different multi-scale feature extraction blocks to extract the joint spatial-spectral features and the advanced spatial features, respectively. Moreover, a spatial-spectral attention module and a spatial attention module were set up to focus on the salient spatial parts and valid spectral information. Experimental results demonstrate that our method achieves high accuracy on the Indian Pines, Pavia University and Salinas datasets. The source code can be found at <https://github.com/XiangdongZ/MSRN-A>.

Keywords: hyperspectral image classification; convolutional neural network; multi-scale features extraction; attention mechanism

## 1. Introduction

Hyperspectral images (HSIs) not only reflects the spatial distribution information of surface objects, but also contains abundant spectral information (Li et al. 2019). As an image-spectrum merging technology, hyperspectral imaging has been widely used in various fields such as environmental detection (Yang and Yu 2017) and agricultural monitoring (Liang et al. 2015). HSI classification plays an important role in these fields, its purpose is to determine a unique category identification for each image pixel.

With the rapid development of deep learning in recent years, HSI classification methods based on convolutional neural network (CNN) have become a research hotspot. For example, (Makantasis et al. 2015) exploited a 2D-CNN to encode pixels' spectral and spatial information and a Multi-Layer Perceptron (MLP) to conduct the classification task.

A 3D-CNN framework was proposed to extract the deep spectral–spatial-combined features without relying on any preprocessing or post-processing (Li, Zhang, and Shen 2017). (Roy et al. 2019) proposed a hybrid CNN composed of continuous 3D-CNN and 2D-CNN, which can extract the joint spatial-spectral feature and more abstract level spatial feature. In order to solve the problem of network degradation in the CNN model, (Zhong et al. 2017) designed an end-to-end spectral-spatial residual network (SSRN). Motivated by SSRN, (Wang et al. 2018) proposed a fast dense spectral-spatial convolution (FDSSC) framework to reduce the training time and improve accuracy. The above methods have achieved good performance in the HSI classification task.

However, hyperspectral images have significant features that contain rich spatial and spectral information, how to make full use of the abundant information in hyperspectral images for accurate classification is still challenging. In this letter, we propose an end-to-end network called MSRN-A that mainly composed of multi-scale feature extraction blocks and attention modules (Figure 1). On the one hand, the multi-scale feature extraction block combines the Inception architecture (Szegedy et al. 2016) with residual connections (He et al. 2016), which can increase the width and depth of CNN at the same time. Moreover, filters of different size used in the Inception architecture can achieve multi-scale feature extraction. On the other hand, the usage of invalid spatial and spectral information may introduce noises and weaken the performance of deep learning models (Mou and Zhu 2019). Recently, the attention mechanism has achieved amazing performance in computer vision tasks (Hu et al. 2018). Inspired by this, we set up attention modules to focus on informative spectral bands and salient feature in spatial neighbour region. The experiment results demonstrate that the combination of multi-scale feature extraction blocks and attention mechanism can significantly improve the performance and robustness of HSI classification.

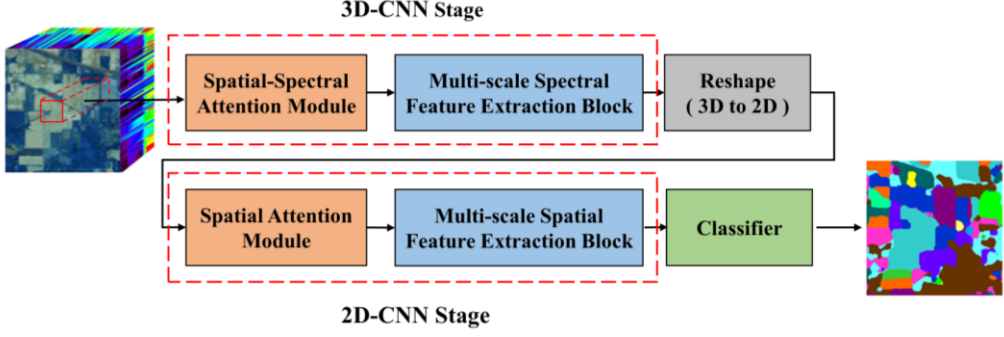


Figure 1. The overall structure of the proposed MSRN-A model for HSI classification.

## 2. Methods

### 2.1 Extracting multi-scale features

As shown in Figure 2, we build the multi-scale spectral feature extraction (MS-Spe-FE) block and the multi-scale spatial feature extraction (MS-Spa-FE) block respectively. In the MS-Spe-FE block, we use filters with sizes of  $3 \times 3 \times 3$ ,  $3 \times 3 \times 5$  and  $3 \times 3 \times 7$ , which can extract joint spatial-spectral features while extracting multi-scale spectral features. Then, the concatenate operation realizes the connection of the generated feature maps of different scales. Finally, the spliced feature map is fused by  $1 \times 1 \times 1$  convolution to complete the fusion of multi-scale spectral features. Similarly, the MS-Spa-FE block was built to extract more advanced and abstract multi-scale spatial features.

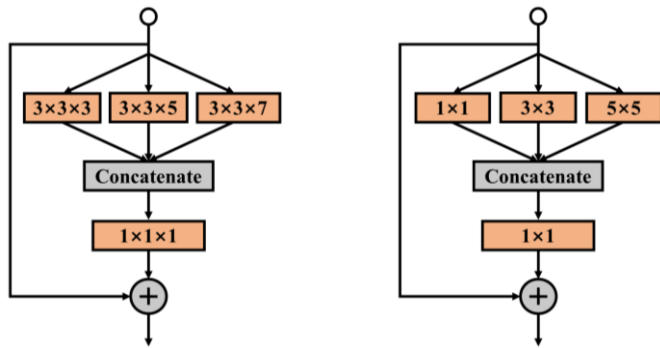


Figure 2. MS-Spe-FE Block (left) and MS-Spa-FE Block (right).

### 2.2 Attention module

(Woo et al. 2018) have proposed Convolutional Block Attention Module (CBAM) to focus on important features and suppressing unnecessary ones along the channel and

spatial axes. The use of extra spatial and spectral information in the HSI classification process may introduce noises, therefore, we add attention mechanism to the existing classification network to focus on salient spatial part and informative spectral bands. In the 3D-CNN stage, we propose the spatial-spectral attention (SSA) module to generate the spatial-spectral feature refinement maps (Figure 3).

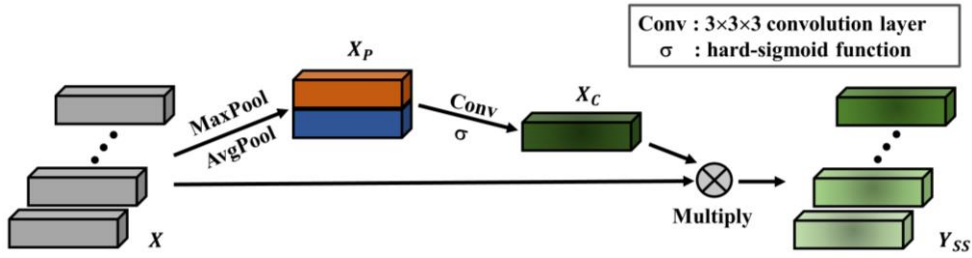


Figure 3. Spatial-spectral attention (SSA) module.

In the proposed SSA module, we first use both max-pooling and average-pooling operations along the channel axis and concatenate them to preserve texture and background information to the greatest extent. Then, we apply a standard convolution layer with the hard-sigmoid activation function to generate attention maps, which denote the silent part in the spatial neighbor region and informative band among hundreds of spectral bands. In the end, the generated attention maps are multiplied to the input feature map for adaptive feature refinement.

In the 2D-CNN stage, we design the spatial attention (SA) module to generate the more abstract spatial feature refinement maps (Figure 4). The overall process of SA module is similar to SSA module. The difference is that the SA module uses a  $3 \times 3$  convolution instead of  $3 \times 3 \times 3$  convolution.

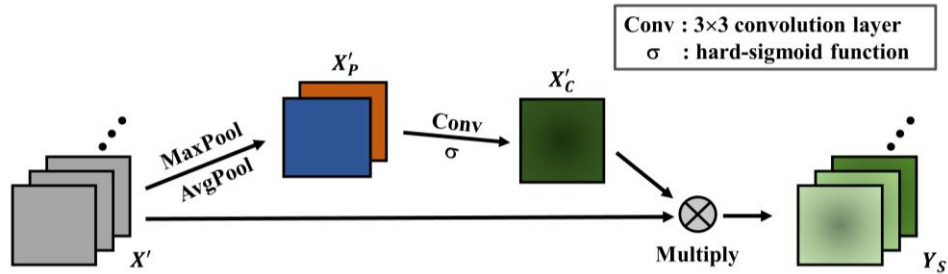


Figure 4. Spatial attention (SA) module.

### 3. Experiments and analysis

All the experiments are conducted on the Keras deep learning platform with the Tesla V100 GPU (32GB RAM). In order to objectively evaluate the performance of different methods in the experiments, the overall accuracy (OA), average accuracy (AA), and kappa coefficient ( $k$ ) are used as the evaluation indicators of classification accuracy.

#### 3.1 Experimental datasets

To evaluate the performance of the proposed method, we use three public datasets in the experiments, namely, the Indian Pines (IN) dataset, the Pavia University (UP) dataset and the Salinas (SA) dataset. In the experiment, each dataset is divided into three groups: the training set, the validation set and the test set. We randomly select 200 samples as the training set, 100 samples as the validation set and the rest as the test set in each category. For categories that less than 400 samples in the IN dataset, the ratio of the training set, validation set and test set is 2:1:7.

#### 3.2 Network configuration

In the proposed MSRN-A model, we use the RMSprop optimizer to optimize the loss function, and choose a small learning rate of 3e-04. A learning rate decay strategy is adapted to speed up the convergence of the network. In addition, we utilize early stopping in the training process and add dropout before the fully connected layer to prevent overfitting. Since some parameters have significant impact on the performance of the network, it is necessary to determine the appropriate value of these parameters through comparative experiments.

##### 3.2.1 Kernel Numbers

The number of convolution kernels decides the representation capacity and computation

of the proposed network. We set different kernel numbers from 16 to 32 at regular intervals to find an optimal network that balances performance and speed. As shown in Figure 5, the number of convolution kernels in the optimal model corresponding to the three datasets (IN, UP, and SA) is 28, 24 and 32, respectively.

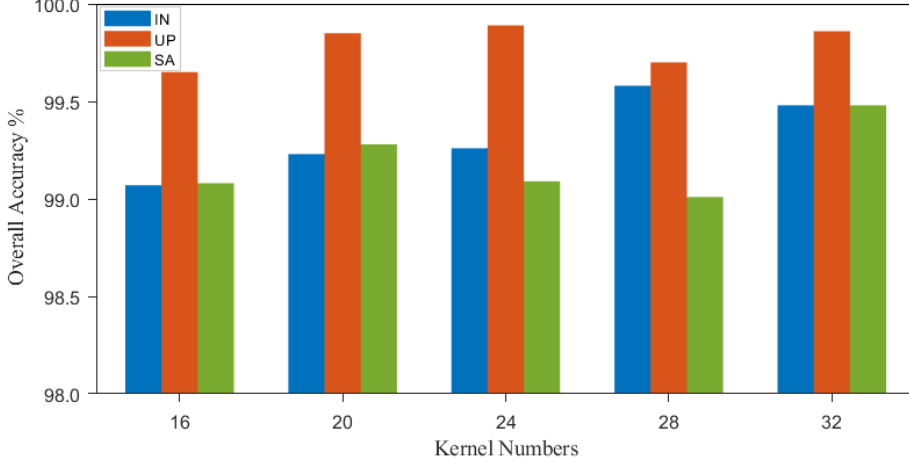


Figure 5. OA (%) of the MSRN-A model with different kernel numbers in the IN, UP, and SA datasets.

### 3.2.2 Spatial size

The size of the spatial neighbor region affects the performance and speed of MSRN-A model to a certain extent. Larger spatial size provides more spatial information, but it may also introduce noises and reduce the training speed of the model. To find the best spatial size for each dataset, we test the proposed model with different sizes (Table 1). As shown in Table 1, the optimal spatial size for the IN and UP datasets is  $15 \times 15$ , for the SA dataset is  $17 \times 17$ , respectively.

Table 1. OA (%) and training time for different spatial size in the IN, UP, and SA datasets.

Spatial size	Indian Pines		Pavia University		Salinas	
	OA (%)	Training time (s)	OA (%)	Training time (s)	OA (%)	Training time (s)
$9 \times 9$	98.66	520.25	99.47	200.81	98.05	596.22
$11 \times 11$	99.13	562.46	99.66	248.50	99.06	838.41
$13 \times 13$	99.38	713.73	99.85	323.13	98.82	704.83
$15 \times 15$	99.56	858.68	99.87	371.65	99.67	903.19
$17 \times 17$	99.43	1112.53	99.78	399.12	99.85	1048.68

### 3.2.3 Arrangements of the attention module

Since the attention modules and the multi-scale feature extraction blocks play different roles in the MSRN-A model, we test the proposed model with three different arrangements of the SA and SSA attention module to find the best strategy (Figure 6).

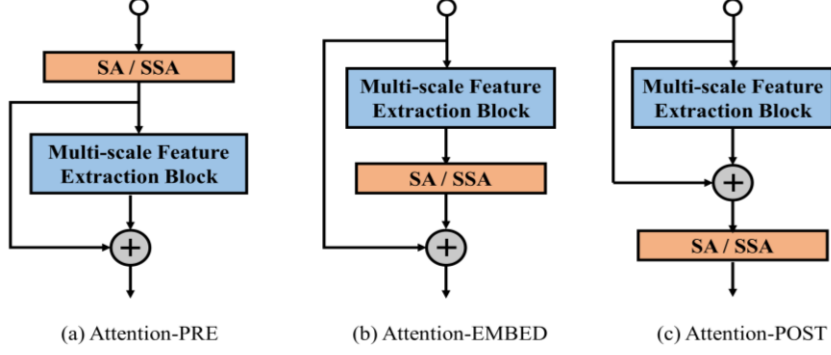


Figure 6. Arrangements of the SA and the SSA module.

Table 2 summarizes the classification accuracies of different attention strategy. The results show that different attention arrangements have a slight influence on the classification performance of the MSRN-A model. As plug-and-play modules, SA and SSA can be integrated into any location in existing network for HSI classification to improve their performance.

Table 2. Classification accuracies of different attention strategy.

Strategy	Indian Pines			Pavia University			Salinas		
	OA (%)	AA (%)	$k$ ( $\times 100$ )	OA (%)	AA (%)	$k$ ( $\times 100$ )	OA (%)	AA (%)	$k$ ( $\times 100$ )
PRE	99.13	99.18	98.87	99.88	99.87	99.84	99.46	99.82	99.40
EMBED	99.37	98.75	99.27	99.80	99.66	99.73	99.67	99.87	99.63
POST	99.37	98.71	99.25	99.83	99.85	99.78	99.51	99.83	99.45

### 3.3 Experimental results

To demonstrate the effectiveness of the proposed MSRN-A model, we compare it with advanced deep learning methods such as 2D-CNN and 3D-CNN, and state of the art models such as SSRN and FDSSC. In addition, we also tested the MSRN model that do not contain the SA and SSA module to reflect the powerful capacity of the attention mechanism.

Table 3. Classification accuracies of different methods for the IN, UP, and SA datasets. Bold indicates the best result.

Methods	Indian Pines			Pavia University			Salinas		
	OA (%)	AA (%)	$k$ ( $\times 100$ )	OA (%)	AA (%)	$k$ ( $\times 100$ )	OA (%)	AA (%)	$k$ ( $\times 100$ )
2D-CNN	87.27	84.35	85.10	96.04	96.57	94.66	95.79	98.30	95.28
3D-CNN	94.04	91.14	93.01	94.13	95.00	92.11	93.46	97.37	92.67
SSRN	98.74	86.52	98.52	99.77	99.68	99.69	99.57	99.82	99.52
FDSSC	99.17	<b>99.52</b>	99.02	<b>99.92</b>	<b>99.96</b>	<b>99.88</b>	98.26	99.42	98.05
MSRN	99.42	99.22	99.31	99.74	99.75	99.65	99.76	99.87	99.73
MSRN-A	<b>99.64</b>	99.10	<b>99.58</b>	99.91	99.83	<b>99.88</b>	<b>99.96</b>	<b>99.94</b>	<b>99.95</b>

It can be observed from Table 3 that the MSRN-A model achieve the highest classification accuracy on the IN and SA datasets. In the UP dataset, the OA and AA of our method are slightly lower than FDSSC, but has the same value of  $k$ . What's more, the MSRN model outperforms 2D-CNN, 3D-CNN, and SSRN in all three datasets, which demonstrate that the multi-scale feature extraction blocks can fully utilize the spatial and spectral information. Considering that the MSRN model removes the SA and SSA modules, and its classification accuracy is lower than the MSRN-A model. It can be proved that the attention mechanism helps the network to focus on important information and suppress unnecessary noises.

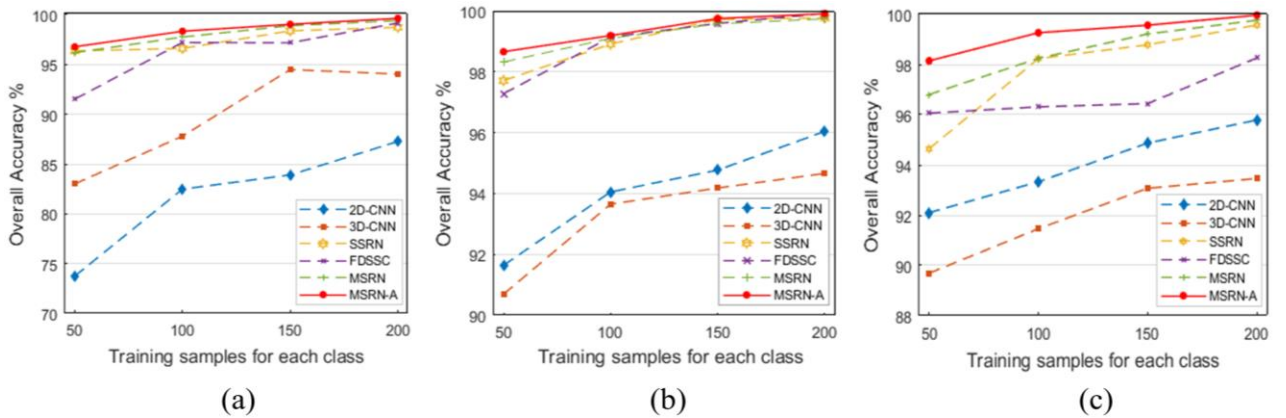


Figure 7. OA (%) of different methods with different training sample number per class on three datasets. (a) IN. (b) UP. (c) SA.

As shown in Figure 7, When gradually reducing the number of training samples, the OA of all methods is also decreasing to varying degrees. However, the MSRN-A model

still achieve high classification accuracy with a small number of training samples per class, while the accuracy of compared methods is greatly reduced.

#### 4. Conclusions

In this letter, we present an efficient deep learning framework for HSI classification. The proposed MSRN-A model, mainly consists of multi-scale feature extraction blocks and attention modules, which can take full advantage of the useful information in HSIs. Experimental results show that the proposed model has achieved high classification accuracy with limited training data. Finally, the proposed attention modules can be used as plug-and-play modules for existing networks to improve their performance.

#### Acknowledgements

The authors thank all distinguished reviewers for their suggestions on this letter.

#### Funding

The project is jointly funded by basic scientific research business of Central University of Chang'an University (No.300102269205, No.300102269304), National Key R&D Program of China (No.2018YFC1504805, No.2019YFC1509201).

#### References

Li, S., W. Song, L. Fang, Y. Chen, P. Ghamisi, and J. A. Benediktsson. 2019. "Deep learning for hyperspectral image classification: An overview." *IEEE Transactions on Geoscience and Remote Sensing* 57(9): 6690-6709. doi:10.1109/TGRS.2019.2907932.

Yang, X., and Y. Yu. 2017. "Estimating soil salinity under various moisture conditions: An experimental study." *IEEE Transactions on Geoscience and Remote Sensing* 55(5): 2525-2533. doi:10.1109/TGRS.2016.2646420.

Liang, L., L. Di, L. Zhang, M. Deng, Z. Qin, S. Zhao, and H. Lin. 2015. "Estimation of crop LAI using hyperspectral vegetation indices and a hybrid inversion method." *Remote Sensing of Environment* 165: 123-134. doi: 10.1016/j.rse.2015.04.032.

Makantasis, K., K. Karantzalos, A. Doulamis, and N. Doulamis. 2015. "Deep supervised learning for hyperspectral data classification through convolutional neural

networks." *2015 IEEE International Geoscience and Remote Sensing Symposium*, 4959-4962. doi: 10.1109/IGARSS.2015.7326945.

Li, Y., H. Zhang, and Q. Shen. 2017. "Spectral–spatial classification of hyperspectral imagery with 3D convolutional neural network." *Remote Sensing* 9(1): 67. doi: 10.3390/rs9010067.

Roy, S. K., G. Krishna, S. R. Dubey, and B. B. Chaudhuri. 2019. "HybridSN: Exploring 3-D–2-D CNN Feature Hierarchy for Hyperspectral Image Classification." *IEEE Geoscience and Remote Sensing Letters* 17(2): 277-281. doi: 10.1109/LGRS.2019.2918719.

Zhong, Z., J. Li, Z. Luo, and M. Chapman. 2017. "Spectral–spatial residual network for hyperspectral image classification: A 3-D deep learning framework." *IEEE Transactions on Geoscience and Remote Sensing* 56(2): 847-858. doi: 10.1109/TGRS.2017.2755542.

Wang, W., S. Dou, Z. Jiang, and L. Sun. 2018. "A fast dense spectral–spatial convolution network framework for hyperspectral images classification." *Remote Sensing* 10(7): 1068. doi: 10.3390/rs10071068.

Szegedy, C., V. Vanhoucke, S. Ioffe, J. Shlens, and Z. Wojna. 2016. "Rethinking the inception architecture for computer vision." *Proceedings of the IEEE conference on computer vision and pattern recognition*, 2818-2826. doi: 10.1109/CVPR.2016.308.

He, K., X. Zhang, S. Ren, and J. Sun. 2016. "Deep residual learning for image recognition." *Proceedings of the IEEE conference on computer vision and pattern recognition*, 770-778. doi: 10.1109/cvpr.2016.90.

Hu, J., L. Shen, and G. Sun. 2018. "Squeeze-and-excitation networks." *Proceedings of the IEEE conference on computer vision and pattern recognition*, 7132-7141. doi: 10.1109/cvpr.2018.00745.

Mou, L., and X. X. Zhu. 2019. "Learning to Pay Attention on Spectral Domain: A Spectral Attention Module-Based Convolutional Network for Hyperspectral Image Classification." *IEEE Transactions on Geoscience and Remote Sensing* 58(1): 110-122. doi: 10.1109/TGRS.2019.2933609.

Woo, S., J. Park, J. Y. Lee, and I. So Kweon. 2018. "Cbam: Convolutional block attention module." *Proceedings of the European Conference on Computer Vision*, 3-19. doi: 10.1007/978-3-030-01234-2\_1.